The April-May 2006 volcano-tectonic events at Stromboli volcano (Southern Italy) and their relation with the magmatic system.

Luca D'Auria, Flora Giudicepietro, Marcello Martini and Massimo Orazi
Istituto Nazionale di Geofisica e Vulcanologia
sezione di Napoli, Osservatorio Vesuviano

July 28, 2006

Abstract

Between April 10th and May 22th 2006, a small seismic swarm of 5 volcano-tectonic events occurred on the volcanic island of Stromboli (Southern Italy). Two of these, having $M > 3$ and an intensity of about V-VI MCS, were clearly felt causing concern in the population. They were recorded during a period of increased explosive activity and were followed by two major explosions at the summit craters on May 22th, few hours after the last earthquake and on 16th June. The location of such events has been performed using a probabilistic approach based on the Equal Differential Time tecnique. Using this tecnique, we were able to locate all the events, showing how they cluster below the volcanic edifice at a depth of about $5 \div 6$ km. From observed P wave polarities we determined the focal mechanisms of the 4 major events. Using earthquake scaling laws, we calculated the fault area and the average slip for the two major events. Finally, assuming an homogeneous half-space model we computed the isotropic stress changes below the volcano edifice. The negative stress variation over the central axis of the volcano suggests that the earthquakes were triggered by a pressurization of the magmatic system.

1 The April-May 2006 seismic swarm

Stromboli is among the most active volcanoes of the world. Its continuous mildly explosive activity is sometimes interrupted by lava effusions and by major explosions [1]. The occurrence of volcano-tectonic events at Stromboli, is not a usual feature, compared with other volcanoes. The last swarm recorded in the area occurred in June 1999 [5]. It was composed of small magnitude events ($M \leq 3.2$) located about 6 km North of the island, none of them was felt. The last earthquake, located close to the island and having a macroseismic intensity higher than V occurred in 1967 (see Table 5).

The 5 volcano-tectonic (VT) events recorded between April 10th and May 22th 2006 (see Table 5) show clear P and S phases, indicating a shear mechanism. This contrasts with seismicity usually recorded at Stromboli that consists of explosion-quakes and Very-Long-Period (VLP) events related to the strombolian activity at the summit craters [7]. The Peak Ground Acceleration (PGA)

recorded by the station closest to the S.Vincenzo village (STR3) for the strongest event (May 5th) was about 0.011 g and the observed macroseismic intensity was V-VI MCS.

We will show how the events are located close to the deeper parts of the magmatic system and far from the shallow source of the usual volcano seismicity [3] (section 2). On the basis of retrieved hypocenters we computed focal mechanisms (section 3) and stress variations (section 4) showing that a pressurization of the magmatic system is a possible trigger of the swarm. In conclusion we discuss the possible relation of these events with the volcanic activity in the months preceeding the swarm.

2 Hypocenter location

The VT swarm was recorded by a permanent network of 12 broadband digital seismic stations (Fig.5) deployed since January 2003 by INGV. The location of these events is made difficult by the small aperture of the network (less than 3 km) limited to the subaerial part of the volcano, by the azimuthal coverage limited by areas of rough and steep topography and by the low signal/noise ratio due to the persistent background volcanic tremor. For this reason we use a robust probabilistic approach based on the Equal Differential Time (EDT) technique. This tecnique is based on the differences between traveltimes of different phases at the same station or differences between traveltimes at different stations [16]. The original approach was modified by [8] and a probabilistic formulation was proposed by [13]. Each couple of traveltimes allows hypocenters to be located over two hyperbola. In the probabilistic formulation, such hyperbola become regions of maximum probability. Hyperbola from different traveltime couples intersect in a volume, where the true hypocenter is likely to be located. The advantage of the EDT approach is that erroneous outliers do not significantly affect the spatial distribution of the maximum likelihood volume [13]. In this paper we use the definition of [13] for the probability density function:

$$p\left(\mathbf{x}\right) = k \left[\sum_{i=1}^{N} \sum_{j=1}^{i-1} \frac{e^{\frac{\left[\left(t_i^{obs} - t_j^{obs}\right) - \left(t_i^{calc} - t_j^{calc}\right)\right]^2}{\alpha_i^2 + \alpha_j^2}}}{\sqrt{\alpha_i^2 + \alpha_j^2}} \right]^N \tag{1}$$

where α_i is the uncertainty related to the i-th picking and k is a normalization constant.

Usually traveltimes in the previous expression are calculated in a 1D or 3D heterogeneous model. In our case, there is no previous knowledge about the velocity model of Stromboli, to a depth of more than few km. [3] used a P-wave velocity of 3500 m/s for the shallow part of the volcanic edifice. We tested a range of velocities ranging from 3000 m/s to 5500 m/s observing that the lowest residuals are obtained for P-wave velocities around 4500 m/s for all the events. The V_P/V_S ratio was fixed to a standard value of 1.73.

Maximum likelihood hypocenters for the p.d.f. (1) were obtained through a search over a grid haning a volume of $6 \times 6 \times 8$ km and a step of 100 m. Hypocenters are shown in Table 5 and in Fig.5. Most of the events are concentrated in the SW sector of the volcano, beneath the village of Ginostra at

depths ranging from 4.7 km to 6.4 km. The only exception is the small event of April 10th having a more shallow hypocenter. The quality of hypocenters is confirmed also by the analisys of first-arrival particle motions (Fig. 5).

From the p.d.f. (1) we can retrieve also statistical estimators of the hypocenter uncertainty. Here we use simply the RMS for each spatial coordinate:

$$RMS\left(x_i\right) = \sqrt{\int_V \sigma\left(\mathbf{x}\right)\left(x_i - \overline{x}_i\right)^2 dV}, \tag{2}$$

where $\overline{x}_i$ is the mean value for each coordinate. Uncertainty for each location are reported in Table 5 and depicted in Fig. 5.

3 Fault plane determination

Hypocenters in Fig.5 are clearly located close to the central axis of the Stromboli volcano. The depth extent of its magmatic system is known only by petrology. There seems to be indications of the existence of magma chambers to depth of $3 \div 12$ km [1] [9]. We investigated the mechanism of the seismic events for inferring about the stress state existing at such depths.

Using a trial and error approach we were able to compute focal mechanisms for the strongest 4 events (Table 5) (Fig.5). The rake angle of the April 18th event mechanism is poorly constrained (Fig.5). In any case, all the events indicates an almost horizontal tensile axis oriented in a NW-SE direction. This direction disagree with the regional stress regime suggested by focal mechanism of crustal earthquakes occurring in the Stromboli region that show a prevalent N-S tensile stress direction [6].

The reason of this discrepancy may be related to a local stress change induced by the magmatic system [15]. The computed mechanisms indicate a contraction in the NW sector, toward the central axis of the volcano (Fig.5).

4 Stress variations

Following [14] for computing deformations and stresses in a homogeneous half-space for a rectangular fault with arbitrary orientation and slip we need and estimate of the fault area and of the fault slip. We consider a simple models of a square faults having length L and area $A = L^2$.

From [2] (eq.3.102) we have a relation between the magnitude M and the seismic moment M_0:

$$logM_0 = 1.01M + 9.93. \tag{3}$$

For the two major events we estimate the seismic moments as 1.5×10^{13} Nm for the April 18th and 2.3×10^{13} Nm for the May 5th event. The basic relation between the fault area A and the average slip d is:

$$M_0 = \mu A d. \tag{4}$$

We obtain an estimate of the rigidity modulus $\mu = 1.9 \times 10^{10}$ Pa from the S-wave velocity used in section 2 and assuming an average density of 2800 kg/m^3.

The relation between seismic moment M_0, stress drop $\Delta\sigma$, fault length L and average slip d for a strike-slip square fault is [12] (table 9.1):

$$M_0 = \frac{\pi}{2}\Delta\sigma L^3. \tag{5}$$

The stress drop is assumed to 1 $kbar$, a value observed in other italian volcanic areas [10]. Using eq. 4 and eq. 5 we obtain estimates of the fault length and of the average slip (see Table 5).

In our case the choice among the two possible fault planes is not crucial for computing the stress changes because the difference in the stress field between the two cases is significant only very close to the fault. Assuming the EW planes to be the true ones, we computed the isotropic stress change in the crust below the volcano (Fig.5).

It is interesting to note that the maximum theoretical surface displacement in this case is of the order of 10^{-5} m, while the maximum horizontal tilt of 10^{-2} μrad, below the range of detection of common geodetic instrumentation.

5 Discussion

A causal effect between stress fields induced by pressure variations in volcanic conduits is known from a theoretical and an observational point of view [15]. The changes in the isotropic stress field computed for the two main events in the central axis of the volcano (Fig.5) is of the order of $10^4 \div 10^6$ Pa, equivalent to $0.1 \div 10$ bar, indicating that the relation between the earthquake occurrence and a pressure change in the magmatic system is consistent. Along the central axis of the volcano the prevalent variation is negative (Fig.5). This means that the stress field change related to a pressure variation in the magmatic system that would have triggered the quakes should be positive. In other word, as supposed in sec.3 a plausible triggering mechanism is a pressure increase in the plumbing system.

The swarm occurred in a period of increased volcanic activity (Fig.5). On the basis of the focal mechanisms and of the stress changes due to the major events we infer that the swarm is related to a pressure increase in the deeper portions of the plumbing system.

On May 22th at 23:38 GMT a strong explosion occurred at the North crater of Stromboli [4]. It was followed on June 16th at 13:41 GMT by another, stronger explosion. At the time of the writing no other significant changed occurred in the volcano status. The continuous monitoring of Stromboli will reveal how significant are these changes and if they will affect the future behaviour of the volcano.

Addenda

After the writing of this manuscript two more earthquakes were recorded at Stromboli. The first one was recorded on July 4th at 06:54 GMT, had M=1.7 and its hypocenter was close to the one of April 10th. The second was recorded on July 21th at 05:11 GMT with M=1.9. Its hypocenter was deeper, close to the one of May 5th.

References

[1] A. Bertagnini, N. Metrich, P. Landi, and M. Rosi. Stromboli volcano (aeolian archipelago, italy): An open window on the deep-feeding system of a steady state basaltic volcano. *J. Geoph. Res.*, 108 (B7), 2003.

[2] P. Bormann, M. Baumbach, G. Boch, H. Grosser, G. Choy, and J.L. Boatwright. Seismic sources and source parameters. In P. Bormann, editor, *IASPEI New Manual of Seismological Observatory Practice. Volume 1.* GeoForschungsZentrum, Potsdam, 2002.

[3] B. Chouet, P. Dawson, T. Ohminato, M. Martini, G. Saccorotti, F. Giudicepietro, G. De Luca, G. Milana, and R. Scarpa. Source mechanisms of explosions at stromboli volcano, italy, determined from moment-tensor inversions of very-long-period data. *J. Geoph. Res.*, 108 (B1), 2003.

[4] A. Cristaldi and M. Coltelli. Rapporto settimanale sull'attivit eruttiva dello stromboli. 22-28 maggio 2006. Technical Report prot. UFVG2006/055, Istituto Nazionale di Geofisica e Vulcanologia - sezione di Catania, 2006.

[5] S. Falsaperla, S. Alparone, and S. Spampinato. Seismic features of the june 1999 tectonic swarm in the stromboli volcano region, italy. *J. Volc. Geoth. Res.*, 125:121–136, 2003.

[6] S. Falsaperla, G. Lanzafame, V. Longo, and S. Spampinato. Regional stress field in the area of stromboli (italy): insights into structural data and crustal tectonic earthquakes. *J. Volc. Geoth. Res.*, 88:147–166, 1999.

[7] S. Falsaperla and S. Spampinato. Tectonic seismicity at stromboli volcano (italy) from historical data and seismic records. *Earth and Planetary Science Letters*, 173:425–437, 1999.

[8] Y. Font, H. Kao, S. Lallemand, C. Liu, and L. Chiao. Hypocentre determination offshore of eastern taiwan using the maximum intersection method. *Geoph. J. Int.*, 158:655–675, 2004.

[9] L. Francalanci, S. Tommasini, and S. Conticelli. The volcanic activity of stromboli in the 1906-1998 ad period: mineralogical, geochemical and isotope data relevant to understanding of the plumbing system. *J. Volc. Geoth. Res.*, 13:179–211, 2004.

[10] D. Galluzzo, E. Del Pezzo, M. La Rocca, and S. Petrosino. Peak ground acceleration produced by local earthquakes in volcanic areas of campi flegrei and mt. vesuvius. *Annals of Geophysics*, 47(4):1377–1389, 2004.

[11] P. Gasperini and R. Camassi. Catalogo parametrico dei terremoti italiani. versione 1, 1999.

[12] T. Lay and T.C. Wallace. *Modern Global Seismology.* Academic Press, 1995.

[13] A. Lomax. The equal differential time (edt) likelihood function., 2006.

[14] Y. Okada. Internal deformation due to shear and tensile faults in a half-space. *Bull. Seism. Soc. Amer.*, 82(2):1018–1040, 1992.

[15] D. C. Roman. Numerical models of volcanotectonic earthquake triggering on non-ideally oriented faults. *Geoph. Res. Lett.*, 32, 2005.

[16] H. Zhou. Rapid three-dimensional hypocentral determination using a master station method. *J. Geoph. Res.*, 99 (B8):15439–15455, 1994.

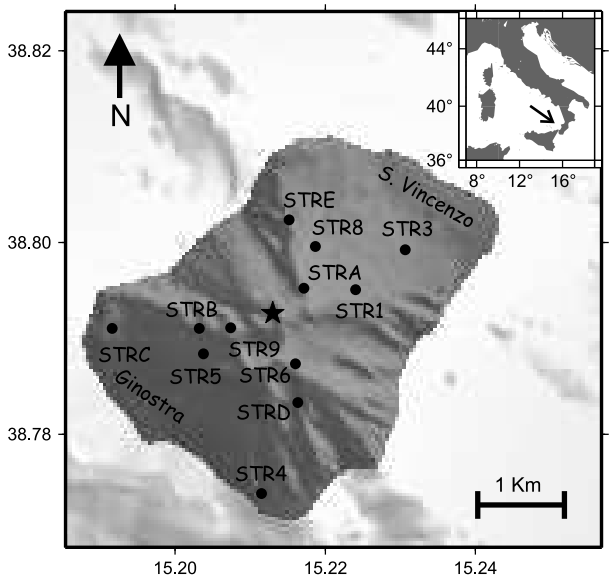

Figure 1: Map of Stromboli island. The upper right inset shows a map of Italy with the position of Stromboli marked by the arrow. Circles are broadband seismic stations. The star marks the position of the summit active craters.

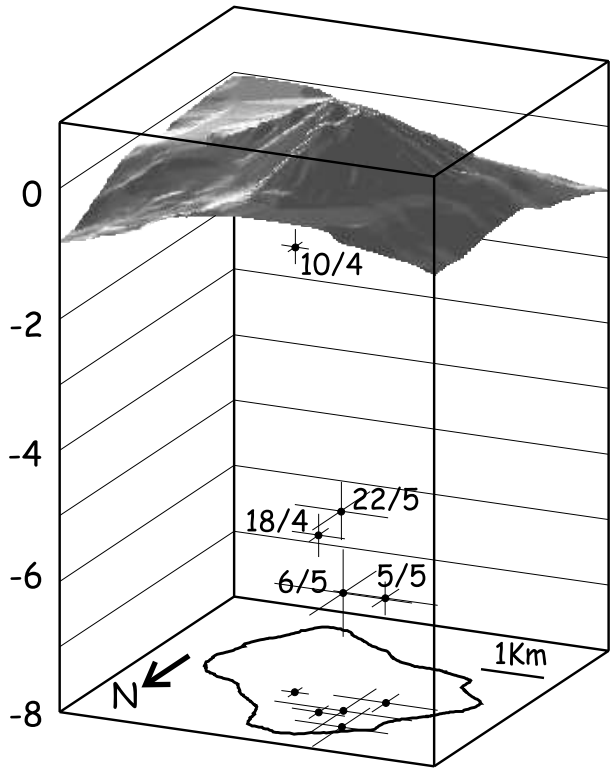

Figure 2: 3D view of hypocenters (black circles) with their error bars. On the bottom there is the horizontal projection of epicenters with error bars. Close to each event, the date of occurrence is indicated.

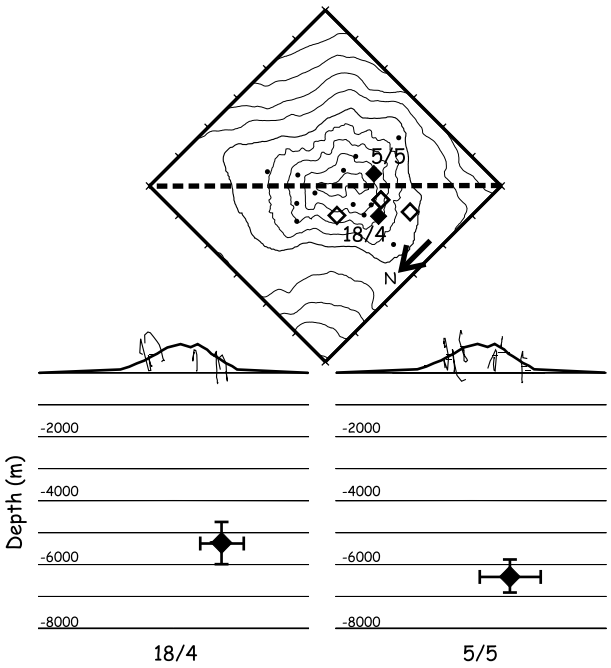

Figure 3: Vertical cross sections along a NE-SW direction (dashed line on the map). Black circles on the map are station positions, white diamonds are epicenters of the 3 weakest events, while black diamonds are epicenters of the two strongest ones. First arrivals particle motion for some stations are represented for the strongest events of April 18th and May 5th. Below there are cross-sections with hypocenters and 2σ error bars. In both cases it is evident how they fit well with hypocenters.

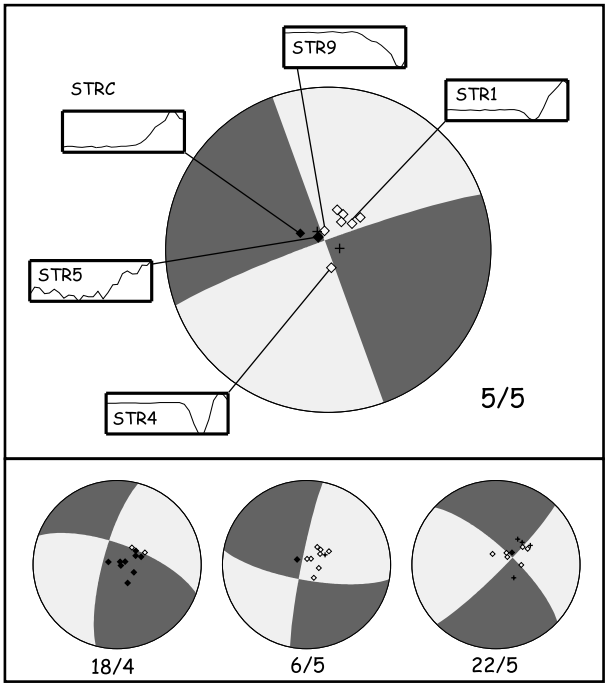

Figure 4: Focal mechanisms of the 4 strongest events. Black and white diamonds indicate respectively upward and downward first motion. Crosses indicates doubtful polarities. The mechanism of the strongest event (5/5) is on the top. It is complemented with a detailed view of some vertical component recordings, starting 0.3 s before and terminating 0.2 s after the picked first arrival. Amplitudes are normalized.

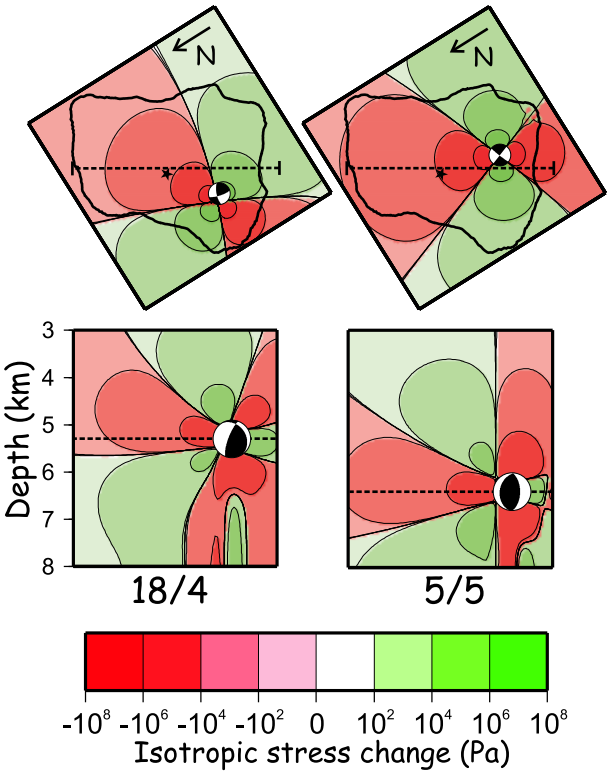

Figure 5: Isotropic stress changes induced by the April 18th and May 5th events. On the top horizontal sections at the depth of the corresponding hypocenter are shown. Stars mark the positions of the summit craters. Below there are vertical cross sections (along the traces indicated in the maps) representing the stress field from 3 to 8 km depth.

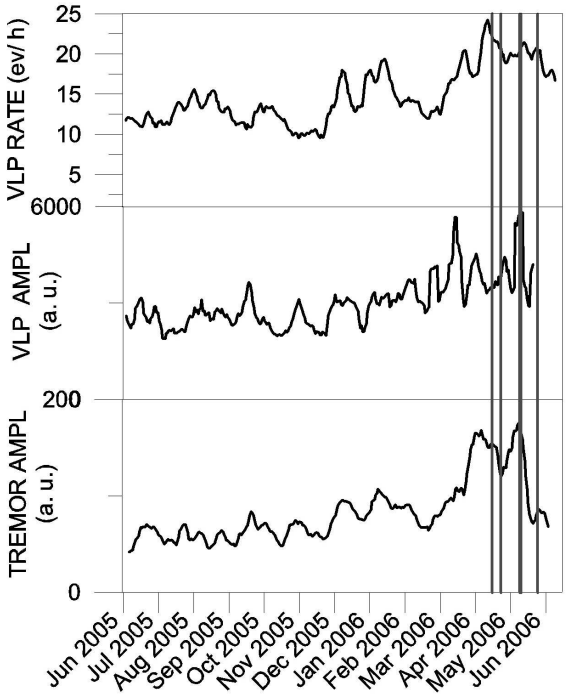

Figure 6: Time evolution of volcanic seismicity at Stromboli from June 2005 to June 2006. On the top there is the average hourly occurrence of VLP events. In the middle the amplitude of the strongest VLP events for each day. On the bottom there is the average volcanic tremor amplitude. All the time series were smoothed with a 7 days moving average. The vertical bars marks the occurrence of the earthquakes.

Date	Lat. (N)	Lon. (E)	MCS	M
1906-06-10 01:44	38.812	15.237	IV-V	4.7 ± 0.16
1909-01-03 04:20	38.812	15.237	VI-VII	$\mathit{4.6 \pm 0.49}$
1916-07-03 23:21	38.812	15.237	VI-VII	$\mathit{4.6 \pm 0.49}$
1941-05-22 06:16	38.800	15.230	VII-VIII	$\mathit{4.6 \pm 0.49}$
1948-10-16 12:10	38.800	15.200	VI	$\mathit{4.3 \pm 0.39}$
1967-08-15 07:06	38.800	15.100	??	4.4 ± 0.35

Table 1: Events with MCS≥V since 1900 located within a radius of 10 km from the center of the island ($38^o.79N, 15^o.21E$). Data are from the parametric catalog of italian earthquakes CPTI99 [11]. Magnitudes in italic were obtained from macroseismic data.

Date and time (GMT)	Md	Lat. (N)	Lon. (E)	Depth (km)	RMSx (m)	RMSy (m)	RMSz (m)
10/04 12:28	1.7	38.7953	15.2048	1.2	255	219	268
18/04 19:31	3.2	38.7890	15.2003	5.3	340	427	330
05/05 20:49	3.4	38.7826	15.2096	6.4	476	836	258
06/05 21:09	2.3	38.7862	15.2026	6.2	1156	1101	666
22/05 19:21	2.4	38.7835	15.1946	4.7	994	745	443

Table 2: Hypocentral parameters for all the events. Magnitudes are computed using the duration magnitude $M_d = 1.818log\,(D) - 0.275$ defined in [6]. Durations were computed on recordings of stations STRC (vertical component) since this is the closest to the station STR used by [6] for their magnitude definition.

Event date	18/4	5/5	6/5	22/5
Azimuth	290	250	100	313
Dip	70	85	75	74
Rake	15	0	-5	-7
Moment ($Nm \times 10^{13}$)	1.5	2.3	-	-
Fault length (m)	46	53	-	-
Average slip (m)	0.37	0.43	-	-

Table 3: Fault plane solutions of the 4 major events. For the two major events also inferred fault dimensions and average slip are reported.